Available online at www.sciencedirect.com

ScienceDirect

Energy Procedia 49 (2014) 551 – 559

Energy Procedia

SolarPACES 2013

Modeling and analysis of stress in high temperature molten salt trough receivers

Nolan Viljoen[a,*]

[a]*Research Engineer, SkyFuel, Inc., 18300 West Highway 72, Arvada, CO, USA 80007*

Abstract

SkyFuel has investigated the stresses and deformations occurring in parabolic trough receivers operating at temperatures above 425°C. Operating at these temperatures allows for direct molten salt storage and higher efficiency conversion from thermal to electric energy. However, at these temperatures, the typical stainless steels used in receiver construction are susceptible to chromium carbide precipitation. After the precipitation has occurred, the steel is vulnerable to intergranular corrosion, and the fatigue strength of the steel is reduced. Corrosion increases the stresses in the receiver walls, and the reduced fatigue strength lowers the stress limit where failure will occur. This paper presents the results of an analysis of these stresses and an evaluation of the receiver material at these operating temperatures. It is shown that parabolic trough receivers can be designed to mitigate the negative effects of chromium carbide precipitation and operate above 425°C without risk of premature failure.

Selection and peer review by the scientific conference committee of SolarPACES 2013 under responsibility of PSE AG.
Final manuscript published as received without editorial corrections.

Keywords: CSP Molten Salt Receivers; CSP Receiver Stresses; CSP Receiver Modelling

1. Introduction and background

Molten salt operation allows Concentrating Solar Power (CSP) parabolic troughs to operate at higher operating temperatures, and facilitates direct molten salt storage. The service life of the receivers at higher temperatures has been investigated in this analysis. For the operating conditions described here, the analysis indicates that a receiver has an adequate service life.

* Corresponding author. Tel.: 1-303-330-0276; fax: 1-866-422-1292.
E-mail address: Nolan.Viljoen@SkyFuel.com

doi:10.1016/j.egypro.2014.03.059

The primary steel alloys used in the thermal receivers of parabolic troughs are AISI 300 series stainless steels. This series of stainless steel exhibits good corrosion resistance and strength at elevated temperatures. The alloying element that gives the steel its corrosion resistance is chromium. As long as the concentration of chromium does not drop below 12%, the steel will remain resistant to corrosion. [1] Between 425°C and 870°C, the chromium precipitates into the grain boundary of the stainless steel as chromium carbide. Chromium carbide precipitation depletes the material near the grain boundary of chromium. This makes the stainless steel sensitive to intergranular corrosion. Intergranular corrosion will, over time, reduce the receiver wall thickness, thereby increasing the localized stress from operating loads. Operating between 425°C and 870°C also reduces the fatigue strength of the stainless steel. [3]

Operating stress is caused by the pressure of the molten salt and uneven heating of the receiver. The stress from the pressure is well understood, but the stress from uneven heating is more difficult to quantify. The receiver is subjected to higher concentration of flux on the portion facing the trough than the portion facing away. The portion of the receiver with the higher flux is a higher temperature, and expands more than the portion facing away. The uneven expansion causes bowing and high point stresses where the bowing is resisted near the receiver supports.

To assess the resulting stresses from uneven heating, a three part analysis was performed. First, the flux distribution on the receiver was determined. From the flux distribution, the resulting temperature distribution was derived from known heat transfer behaviour. The resulting temperature distribution was then incorporated into a receiver Finite Element Analysis (FEA) to determine the stresses on the receiver. The reference coordinate system for the analysis is shown in Figure 1 and Figure 2.

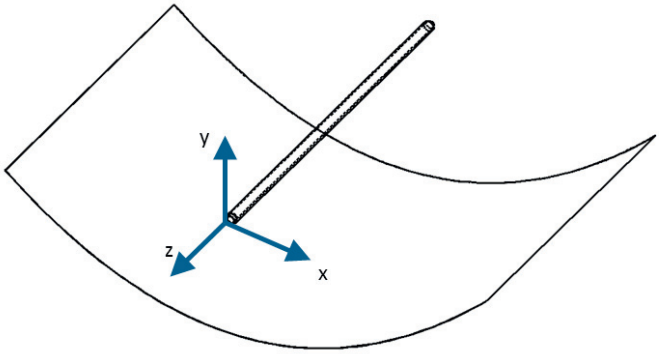

Figure 1. Trough 3-Dimensional Coordinate System

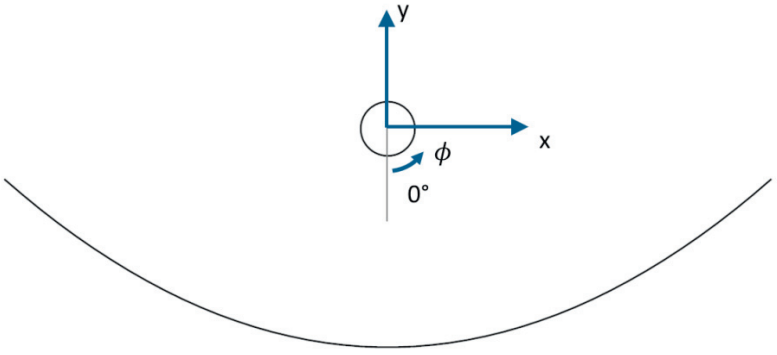

Figure 2. Receiver Angular Position Coordinate System

The molten salt used in the modelling is a solar binary salt with 60% $NaNO_3$ and 40% KNO_3. The properties of this salt can be found in *Solar Power Tower Design Basis Document [11]*.

Nomenclature

r	Radius on Receiver
ϕ	Angular location on receiver
k	Thermal conductivity
$\dot{q}$	Heat absorbed by control volume
$\dot{q}_r$	Flux along r
$\dot{q}_\phi$	Flux along ϕ

2. Flux on the receiver

The flux on the receiver can be determined from using either a ray trace program or an analytical method as described in *Active Solar Collectors and Their Application [10]*. Some ray tracing programs that are available include SolTrace [9] and ASAP [2]. For this paper, an analytical model was constructed and compared to SolTrace results. The model assumed that the optical error can be characterized by a Gaussian distribution with a standard deviation of 5 mrad. Sun shape was also included and was based on published profiles [10]. The rim angle of the collector was fixed at 82.5° and the concentration ratio was varied from 60 to 120. The resulting flux distribution is shown in Figure 3.

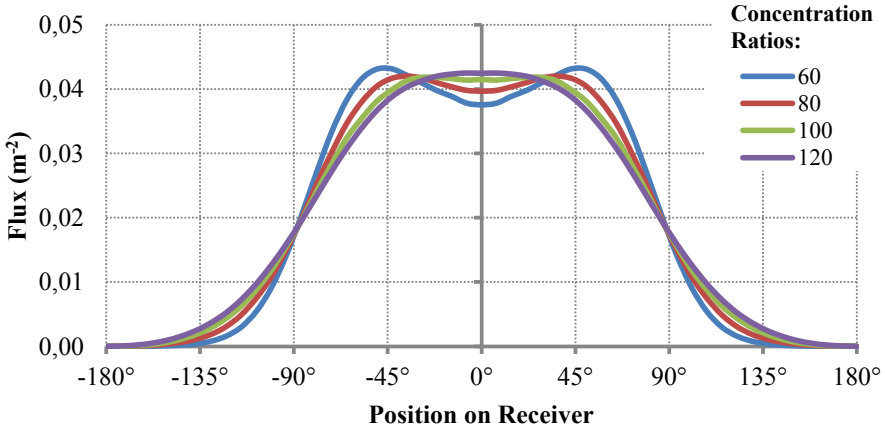

Figure 3. Unit Flux distribution on receiver at different concentration ratios

The flux shown is normalized so that the total flux on the receiver, i.e. the area under the curve, is equal to 1 m-2 to allow adjustment of the distribution for any trough aperture width and Direct Normal Insolation (DNI).

3. Receiver temperature distribution

Once the flux is determined, the circumferential temperature distribution of the receiver wall can be established. Some previous modelling efforts have only considered the temperature distribution along the length of the receiver, but not circumferential [4]. To determine the circumferential distribution, a finite difference model was developed. The model is based on the Heat Equation in cylindrical coordinates:

$$\frac{1}{r}\frac{\partial}{\partial r}\left(kr\frac{\partial T}{\partial r}\right)+\frac{1}{r^2}\frac{\partial}{\partial \phi}\left(k\frac{\partial T}{\partial \phi}\right)+\frac{\partial}{\partial z}\left(k\frac{\partial T}{\partial z}\right)+\dot{q}=\rho c_p\frac{\partial T}{\partial t} \quad (1)$$

[7]

The model is simplified by assuming that heat transfer in the z direction (along the axis of the receiver) is insignificant. Based on this assumption, the heat transfer in the z direction is set to zero and the equation reduces to the following:

$$\frac{1}{r}\frac{\partial}{\partial r}\left(kr\frac{\partial T}{\partial r}\right)+\frac{1}{r^2}\frac{\partial}{\partial \phi}\left(k\frac{\partial T}{\partial \phi}\right)+\dot{q}=\rho c_p\frac{\partial T}{\partial t} \quad (2)$$

where:

$$\dot{q}_r=-k\frac{\partial T}{\partial r} \qquad \dot{q}_\phi=-\frac{k}{r}\frac{\partial T}{\partial \phi} \quad (3)$$

The differential control volume of (2) is shown in Figure 4.

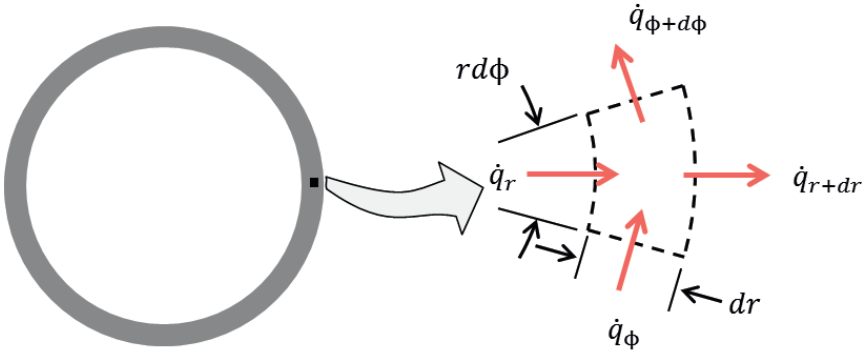

Figure 4. Receiver Temperature Distribution Control Volume

Convection occurs between the molten salt and the receiver's inner wall. Between the inner and outer receiver walls, heat transfer is in the form of conduction. The heat transfer between the outer receiver wall and the glass envelope is modelled as radiation. A high vacuum exists between the receiver and glass envelope; consequently, conduction and convection are neglected. Finally, both conduction and convection occur between the glass envelope and the surrounding air.

The model performs iterative calculations until the temperature change in all of the differential control volumes becomes zero. The circumferential temperature distribution is a function of flow rate, molten salt temperature, and Direct Normal Insolation (DNI). Figure 5 shows temperature distribution along the outer surface of the receiver at peak insolation levels in a trough with a concentration ratio of 80/π. Various flow rates and molten salt temperatures are shown. While lower fluid temperatures produce slightly larger temperature differences around the circumference, the mean wall temperature is higher with higher temperature molten salt. The strength of stainless steel decreases at higher temperatures; consequently, the model results in this paper are presented for the higher temperature molten salt. The magnitude of the displacement, or bow, of the receiver is proportional to the difference between the maximum and minimum temperatures. This difference increases as the flow rate reduces. This is shown in Figure 6 for several concentration ratios.

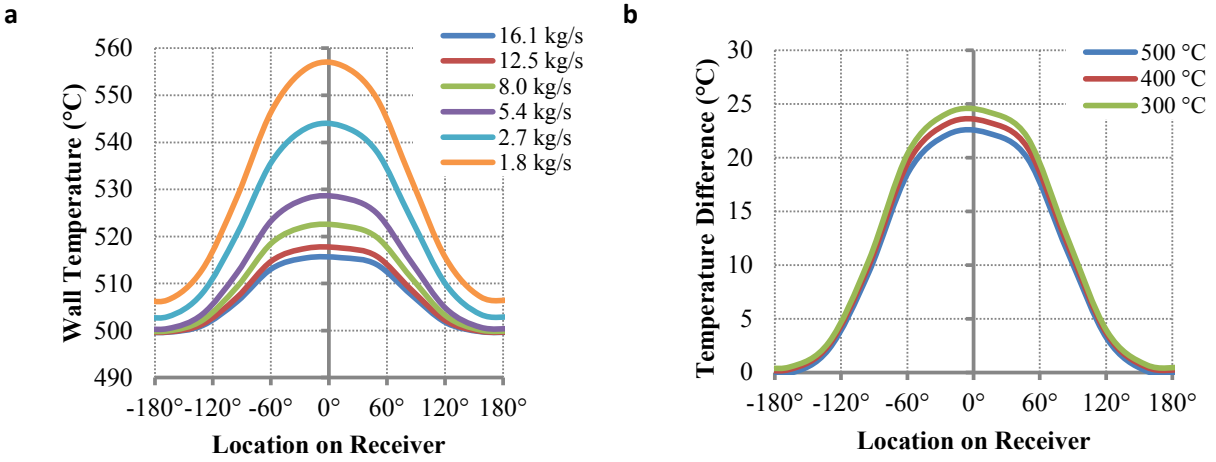

Figure 5. (a) Receiver wall temperature as a function of molten salt flow rate for DNI = 1000 W/m², Receiver Outer Diameter = 90 mm, Concentration Ratio = 80/π, and Fluid Temperature = 500°C; (b) Receiver wall temperature difference (from wall minimum temperature) as a function of molten salt temperature with DNI = 1000 W/m², Receiver Oouter Diameter = 90 mm, Concentration Ratio = 80/π, and Flow Rate = 8 kg/s

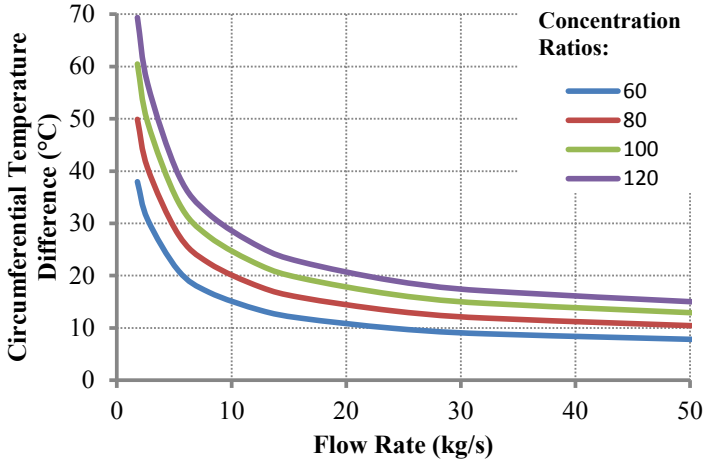

Figure 6. Receiver wall circumferential temperature difference as a function of flow rate for four concentration ratios

As is shown in Section 4, the magnitude of the stress and strain is proportional to the difference between the maximum and minimum temperatures around the circumference of the receiver. This difference increases as the flow rate decreases. This is shown in Figure 6 for several concentration ratios.

4. Receiver FEA model

SolidWorks Simulation is used to perform the Finite Element Analysis (FEA) to model stress in the receiver. The receiver is modelled as a circular tube with the wall represented as a 2 dimensional shell. The trough receiver supports are included in the model to provide the mechanical boundary constraints, and do not allow rotation at the supports. One support does not allow translation, while the second allows translation only along the receiver axis. This translation accommodates the net thermal expansion that occurs as the receiver average temperature rises from ambient to working temperature. The receiver and a trough receiver support are shown in Figure 7a. Figure 7a also shows the location of the peak stress in the receiver.

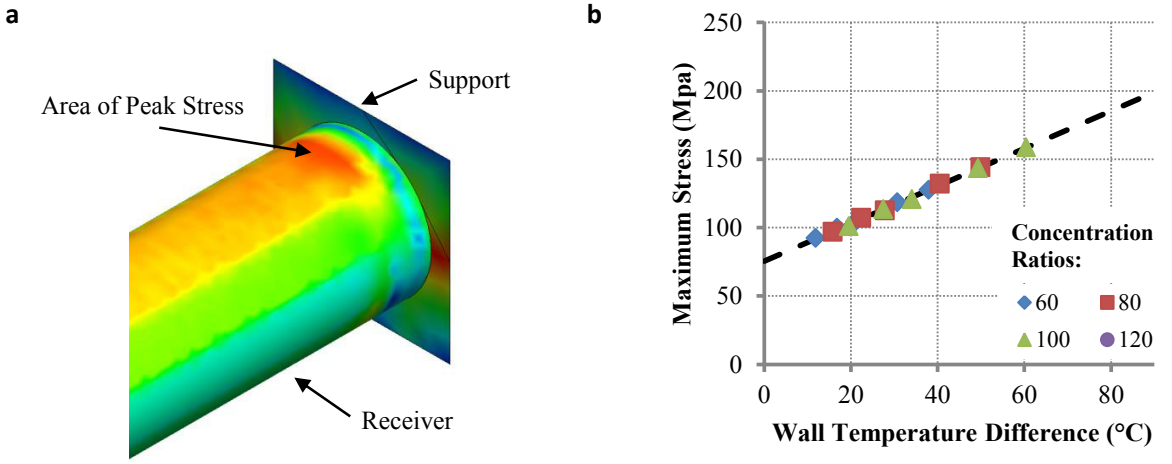

Figure 7. (a) Receiver FEA Model; (b) Maximum stress in a receiver with 90 mm outer diameter, 4.7 m length, and 2.5 mm wall thickness as a function of the difference in temperature between the hot and cold sides of the receiver.

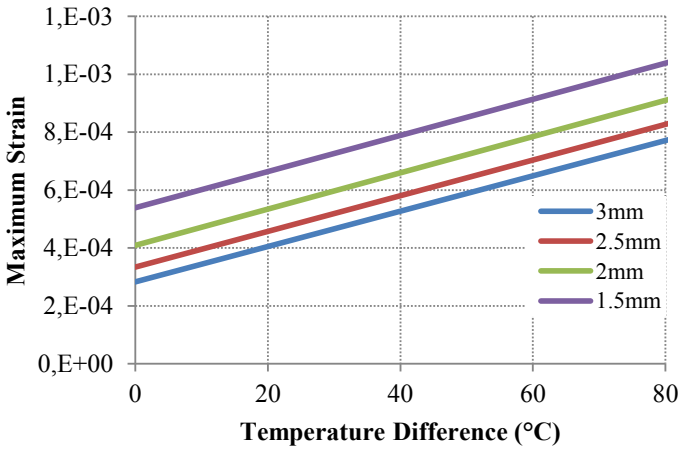

Figure 8. Maximum strain in the wall of a receiver as a function of circumferential temperature difference for four receiver wall thicknesses.

Figure 7b shows that the maximum stress has a linear relation to the temperature difference between the hot and cold sides of the receiver. The strain is also of interest. Figure 8 shows the maximum strain receivers withstand as a function of the receiver wall temperature difference for four receiver wall thicknesses.

5. Receiver service life

The primary material used to make the absorber element of the receiver is AISI 300 series stainless steel. This series of steel is selected for its corrosion resistance and relatively low cost. At temperatures between 425°C and 870°C, the 300 series material will undergo chromium carbide precipitation. Precipitation can be minimized by reducing the concentration of carbon in the steel as in AISI 316L (UNS S31603) stainless steel. As an alternative, additional alloying elements can be added that will form other carbides (instead of chromium carbide). Titanium is used for this purpose in AISI 316Ti (UNS S31635) stainless steel and AISI 321 (UNS S32100) stainless steel. [6]

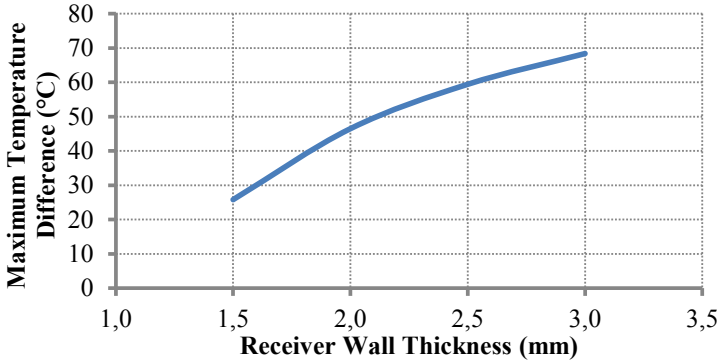

Figure 9. Maximum allowable reciver wall circumferential temperature difference.

Studies have been performed to evaluate the rate of corrosion of various 300 series stainless steels. The corrosion rate of AISI 321 stainless steel in a binary solar salt was 12.3 mg/cm²-yr. [8] Extrapolating this rate out to 30 years, the receiver wall will thin by 0.5 mm. A second study found the corrosion rate for AISI 316 stainless steel in binary salt to be 10.2 mg/cm²-yr. [5] Again extrapolating this out to 30 years, the receiver wall will be reduced by 0.4 mm. The reduction in thickness will increase the stress in the receiver wall.

Chromium carbide precipitation also reduces the fatigue strength of 300 series stainless steel. The ASM handbook defines the allowable strain for AISI 316 stainless steel as 7 x10-4 for 1,000,000 cycles at temperatures not exceeding 510°C. [3] Combining this allowable strain with the results shown in Figure 8 gives the maximum receiver wall temperature difference during normal operating conditions for a given wall thickness. This result is shown in Figure 9.

A generalized collector loop was used to evaluate whether normal operating conditions will cause the receiver to fail. The following parameters were used:

- Receiver Dimensions = 90 mm Outer Diameter x 3 mm Wall thickness x 4.7 m length
- Fluid Outlet Temperature = 500°C
- Service Life = 30 Year
- Receiver Material = AISI 316 Stainless Steel
- Collector Thermal Efficiency = 70%
- DNI = 1000 W/m²
- Binary Solar Salt
- Number of Solar Collector Arrays (SCA) per Loop = 6 SCA’s
- Number of Receivers per SCA = 24 Receivers

The above parameters were also used to determine the required flow rate to maintain a given inlet temperature and outlet temperature. These results are shown in Figure 10a. The flow rates were then used to determine the circumferential temperature difference using the relations shown in Figure 6. Strain was then calculated from Figure 8 based on the temperature differences. The results are shown in Figure 10b. The calculated strains are below the 7x10-4 maximum given in Elevated-Temperature Properties of Stainless Steels. [3]

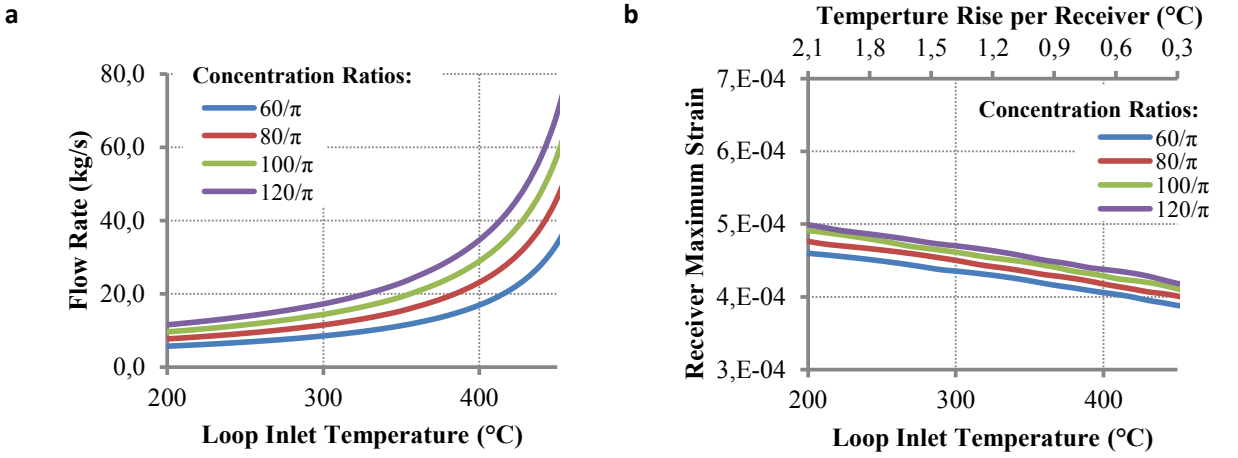

Figure 10. (a) Minimum required flow rate to maintain a 500°C outlet temperature with the given inlet temperature and concentration ratio for a generalized collector loop; (b) The maximum strain in the receivers after 30 years of service as a function of inlet temperature, concentration ratio, and an outlet temperature of 500°C for a generalized collector loop.

The number of Solar Collector Arrays per loop was then reduced to one, to illustrate the impact of a very large temperature increase as molten salt passes through each receiver. These results are shown in Figure 11. The maximum strain does exceed the 7x10-4 maximum for high concentration ratios and temperature rises per receiver.

A 90mm diameter receiver with a wall thickness of 3mm will provide a service life in excess of 30 years on parabolic troughs with a concentration ratio of 80/π, a temperature rise per receiver of less than 10°C, and a molten salt temperature that does not exceed 510°C.

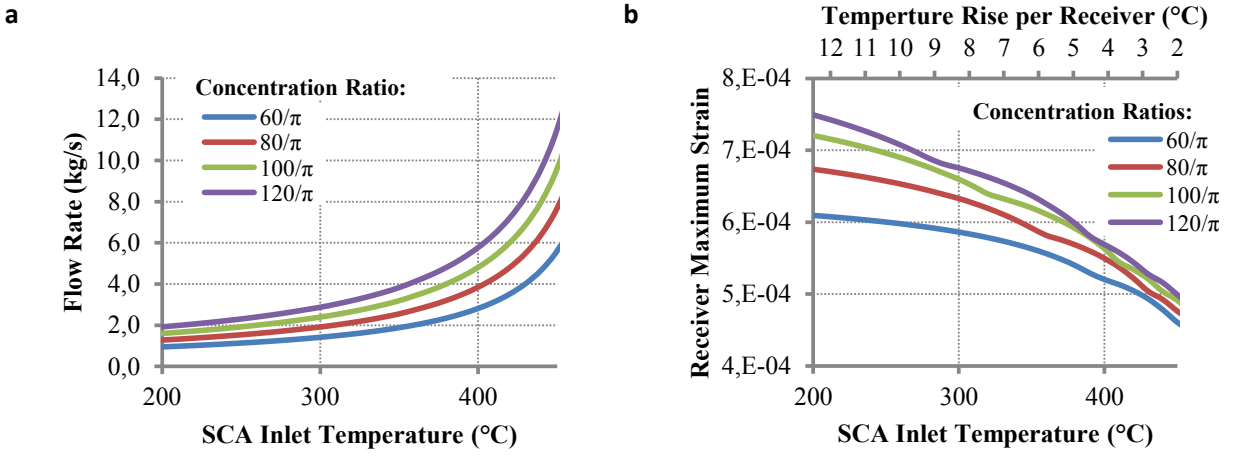

Figure 11. (a) Required flow rate to maintain a 500°C outlet temperature with the given inlet temperature and concentration ratio for a generalized SCA; (b) The maximum strain in the receivers after 30 years of service as a function of inlet temperature, concentration ratio, and an outlet temperature of 500°C for a generalized SCA.

Additional analysis is required to verify the adequacy of receivers for special operating conditions. For example, during fill, the molten salt creates circumferential temperature differences. This impact could be substantially reduced with receiver preheat, particularly if the difference between salt and wall temperatures are less than 50° C. The freezing and thawing of salt in receivers can also exert extremely high stresses that can rupture the receivers. These pressures were not evaluated in this analysis.

The analysis indicates that AISI 300 series molten salt receiver operating at high temperatures as described here, have an adequate service life.

References

[1] Black, J. T., Ronald A. Kohser, and E. Paul DeGarmo. *DeGarmo's Materials and Processes in Manufacturing.* Hoboken, NJ: Wiley, 2008.

[2] Breault Research Organization. *ASAP.* n.d. http://www.breault.com/software/asap.php (accessed May 17, 2013).

[3] *Elevated-Temperature Properties of Stainless Steels.* Vol. 1, in *Properties and Selection: Irons, Steels, and High Performance Alloys*, p. 930-949. ASM International, 1990.

[4] Forristall, R. *Heat Transfer Analysis and Modeling of a Parabolic Trough Solar Receiver Implemented in Engineering Equation Solver.* Technical Report, Golden, CO: National Renewable Energy Laboratory, 2003.

[5] Goods, S. H., R. W. Bradshaw, M. R. Prairie, and J. M. Chavez. *Corrosion of Stainless and Carbon Steels in Molten Mixtures of Industrial Nitrates.* Rep. no. SAND94-8211, Albuquerque, NM: Sandia National Laboratories, 1994.

[6] *High Temperature Characteristics of Stainless Steels.* A Designers' Handbook Series No. 9004, American Iron and Steel Institute, 2011.

[7] Incropera, Frank P., David P. DeWit. *Introduction to Heat Transfer.* New York: Wiley, 1996.

[8] Kruizenga, A. M., and D. D. Gill. "Material Performance of Alloys in NaNO3/KNO3 at 600C." *ECS.* Honolulu, HI: SAND2012-8621P, 2012.

[9] National Renewable Energy Labratory. *SolTrace Optical Modelling Software.* n.d. http://www.nrel.gov/csp/soltrace/ (accessed May 17, 2013).

[10] Rabl, Ari. *Active Solar Collectors and Their Application.* New York: Oxford University Press, 1985.

[11] Zavoico, A. B. *Solar Power Tower Design Basis Document.* SAND2001-2100, Albuquerque, NM: Sandia National Laboratories, 2001.